RSC Advances

ROYAL SOCIETY OF CHEMISTRY

www.rsc.org/advances

Low-Concentration Methane Combustion over Cu/γ-Al_2O_3 Catalyst: Effects of Water

Haojie Geng, Zhongqing Yang, Jingyu Ran, Li Zhang, Yunfei Yan，Mingnv Guo*

Key Laboratory of Low-Grade Energy Utilization Technologies and Systems, Ministry of Education, and College of Power Engineering, Chongqing University, Shapingba District, Chongqing 400030, People's Republic of China.

ABSTRACT: The influence of water on low-concentration methane oxidation over Cu/γ-Al_2O_3 catalyst was investigated in a fixed bed reactor. This paper studied water effect on activity of methane combustion, such as water reversible adsorption, regeneration of the activity and surface characteristics of catalyst. Apparent activation energy was found by experiments, and water surface coverage was computed by Langmuir equation. It was found that the activity of methane combustion over Cu/γ-Al_2O_3 catalyst decreased with time due to water adsorption. The inhibitory effect generated by water was weakened as the temperature rose above 550℃. Reactivity could refresh if the catalyst particles were scavenged by N_2. Kinetic experiment showed that, if water was added into the feed, apparent activation energy (*Ea*) increased obviously (81.4kJ/mol→153.0kJ/mol) and the reaction order with respect to water was -0.6～-1. By Langmuir equation, it could be concluded that the coverage of water adsorption on catalytic active sites increased obviously as vapor was introduced into the feed. If temperature increased, water coverage went down and tended to 0% above 625℃.

KEYWORDS: Cu/γ-Al_2O_3 catalyst; Low-concentration methane; Catalytic combustion; water inhibition

1. INTRODUCTION

There was a large amount of low-concentration methane in the coal bed, especially in China. Conventional combustion technology was hard to make use of them and the gas had no choice but to emit to the atmosphere. Catalytic combustion had been considered to be a comparatively ideal burning mode so far, which could achieve the effect of high-conversion-efficiency and low-pollution-emission with noble metal or transition metal catalyst [1,2,3,4]. A large number of studies had been done on the catalytic combustion of methane with noble or transition metal catalyst, and combustion mechanism had been widely reported [5,6,7]. However the feed always contained a large amount of steam which could affect the reactivity during the actual reaction. Therefore, water effect on methane combustion required further research [8,9,10].

Many catalysts had been investigated for their activity in the catalytic combustion of methane with water over noble catalyst (such as Pd, Pt) and many conclusions was drawn. Some scholars considered that H_2O adsorbed on the active sites, which formed OH* groups, generating inhibitory effects on methane

---

*Corresponding author: Zhongqing Yang, PhD, Associate Professor, Email: zqyang@cqu.edu.cn, Tel: +86 – 023 – 65103114, Fax: +86 –23 –65111832

combustion[11～15]. Among the combustion products, H_2O had an obvious influence than CO_2 in methane combustion. In oxygen-rich condition ($O_2/CH_4 > 2$), it was hard to proceed the reforming reaction of methane with water. About the influence of water, the studies of Ciuparu et al.[16,17] reported that, by means of situ DR-FTIR investigation, several OH adsorption bands were observed on the catalyst surface and hydroxyls were found to related to the PdO phase. OH had bridged and terminal bonds before recombination and desorption as water molecules, suggesting the dehydroxylation mechanism proceeds. Stasinska et al.[18,19] reported that steam could promoted the growth of surface grain, resulting in the decrease of surface area of catalyst. Meanwhile, Qiao et al.[20,21] reported the water vapor could obviously inhibit the catalytic performance of CeO_2-CuO solid solutions for CH_4 and CO conversion, while CeO_2-NiO showed a good resistance to water. By special treatment to ensure differential condition, J.C van Giezen [22] reported that apparent activation energy of methane (*Ea*) increased from 86 kJ/mol to 151 kJ/mol if water was introduced into the feed and the order with respect to water was found to be -0.76.

For methane combustion with water ($O_2/CH_4 > 2$), inhibitory effects of water had been widely acknowledged, especially in Pd or Pt[23～26]. However, there were few studies about transition metal catalyst, such as copper. Water inhibitory effects at low temperature, adsorption characteristics and catalyst surface property were not yet clear in methane combustion. H_2O surface coverage with temperature required further study. The aim of this work was to investigate the water inhibitory effects on the copper based catalyst from the following aspects: water adsorption, regeneration of activity, kinetic parameters of methane and water surface coverage.

2. EXPERIMENT

2.1 Catalyst Preparation and Characterization

γ-Al_2O_3 particles (specific surface area, 181.4m^2/g; pore volume, 0.46cm^3/g; pore diameter, 190.6Å) were used as support to Cu catalyst. γ-Al_2O_3 particle diameter was lower than 0.1mm, and calcined at 500℃ for 6h before loading. Alumina powder was impregnated with the metal using the incipient wetness technique. 0.294g $Cu(NO_3)_2$ powder was choose to load 0.1g Cu on the support(1g). The mass of distilled water, as solvent for $Cu(NO_3)_2$ powder, was determined by the support mass and pore volume. Support particles was impregnated with $Cu(NO_3)_2$ solution for 5h; after impregnation, the catalyst was dried at 150℃ in drying oven for 6h in air and calcined for 6h in muffle furnace at 500℃ in N_2. Self-made catalyst was cooled down to room temperature in muffle furnace (save under N_2 atmosphere). During this process, the nitrate precursor and hydroxyl were completely decomposed and desorbed fully from the catalyst. Table 1 and Table 2 showed the content of each element (XRF) and specific surface area (BET) of the self-made catalyst.

Table 1. The content of each element of Cu/γ-Al_2O_3 catalyst (XRF)

	Cu	Al	O	Si	K	other
Mass(*wt*/%)	9.64%	40.76%	42.98%	1.36%	1.78%	3.84%

Table 2. BET surface area of Cu/γ-Al_2O_3 catalyst

specific surface area	pore volume	pore diameter
180.6m^2/g	0.4571cm^3/g	188.363Å

Fig 1 studied the XRD spectra of Cu/γ-Al_2O_3 catalyst: a, fresh catalyst; b, catalyst after reaction. From Fig 1 (a) and (b), fresh catalyst consisted of CuO and Al_2O_3 between 30° and 70°. Other species (Cu^{1+}, O^{1-}, $O_{2\,ads}$)

were not found in Fig 1. This meant that CuO was the active site that provided O^* (chemisorbed O) to methane. In the flow reactor, as O_2 was enough for CH_4 oxidation ($O_2/CH_4 > 2$), Cu cluster, especially surface Cu, was able to maintain Cu^{2+} and provide O*. Fig 2 (b) showed that, during the reaction, catalyst phrase did not change much, and other peaks were not presented after methane oxidation.

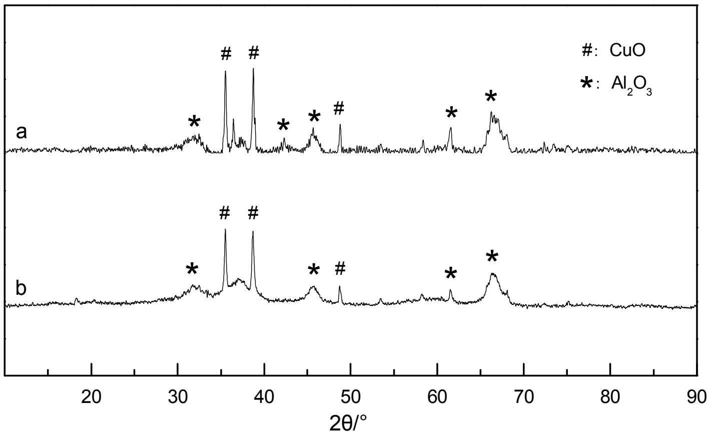

Fig 1. XRD spectra of Cu/γ-Al_2O_3 catalyst

(a) Fresh catalyst; (b) Catalyst after reaction (550℃, 3 *vol.%* CH_4, 20 *vol.%* O_2, N_2 balance)

2.2 Experimental Devices and System

Fig 2 presented the experimental device and system. Experiment of methane combustion was conducted in the fixed-bed reactor which had a ceramic reaction tube with 10mm inner diameter and 1200mm length. The reaction mixture gas (3 vol. % CH_4, 20 vol. % O_2 and N_2 balance) controlled by mass flowmeter, was injected into the fixed-bed reactor at 200ml/min. Water vapor, generated by a vapor generator(W-202A-220-K) was carried by N_2 at 150℃ and mixed with CH_4, O_2 before entering into the reactor. The reactor was heated by resistance-heated furnace that was connected with the data acquisition and control system which controlled the reaction temperature. The effluent gas was measured by gas chromatography to measure the concentration of CH_4 and CO_2.

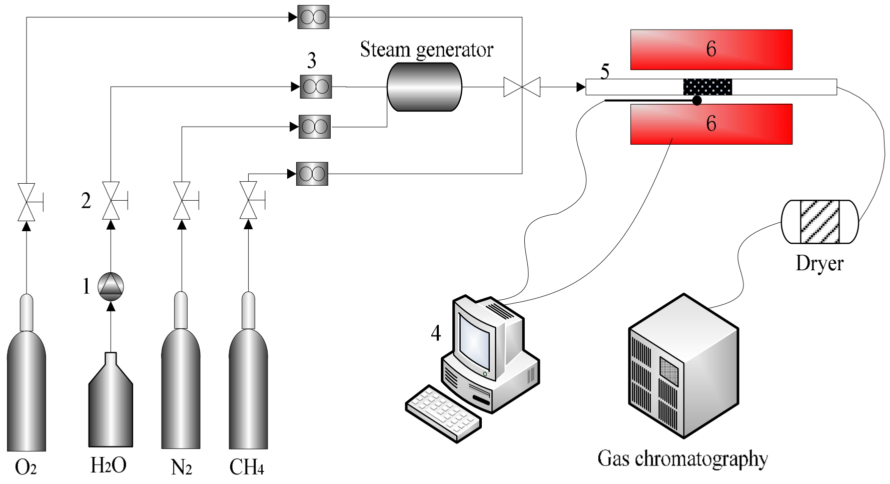

Fig.2 Flow chart of the experimental system

1. Flow Control Pump; 2. Pressure Relief Valve; 3. Mass Flowmeter;
4. Data Acquisition and Control System; 5. Fixed-bed Reactor; 6. Resistance Stove

2.3 Catalytic Activity Test for Methane Oxidation

The reactivity of Cu/γ-Al_2O_3 was determined by methane conversion. According to carbon balance, methane conversion x was described as:

$$x = \frac{[CO_2]}{[CO_2]+[CH_4]} \quad (1)$$

Where $[CO_2]$ and $[CH_4]$ denoted volume percentage of carbon dioxide and methane in the stream.

The microstructure and characterization of catalyst surface were investigated by scanning electron microscope (SEM), which magnified the catalyst surface by 1000 times. BET surface area, pore volume and pore diameter were measured by the BET method before or after the experiments.

3. RESULTS AND DISCUSSION

3.1 Effects of Water on Methane Combustion

Water effect on the methane combustion over Cu/γ-Al_2O_3 catalyst was shown in Fig 3 and Fig 4. Fig 3 showed the change of methane conversion with temperature at different water content (0 *vol*.%, 2.5 *vol*.%, 5 *vol*.%, 10 *vol*.%, 15 *vol*.%, 20 *vol*.%). Fig.4 showed the inhibitory effect of water in methane combustion at 500℃ and 600℃. From these figures, water significantly affected catalytic activity and CH_4 conversion dropped if water was introduced into the feed. When the water vapor increased from 0 *vol.* % to 10 *vol.* %, the catalyst continued losing activity with time. From Fig 3, with temperature rising from 475℃ to 600℃, CH_4 conversion increased quickly. H_2O inhibition on methane combustion increased firstly and then decreased, and water inhibition among the curves reached its maximum at 525℃. The process showed that water vapor had a significantly inhibitory effect on methane combustion, while, with temperature increasing, the influence was weakened gradually. A considerably higher temperature was most likely required for the catalytic reaction.

Differently with Pd and Pt catalyst, Cu catalyst displayed a stronger resistance property to water and could maintain a stable activity at high steam pressure. For the inhibitory effect of water vapor, it was generally considered that water species could adsorbed on the catalyst surface, and reacted with chemisorbed O (O^*): $H_2O + O^* \to OH^*$. Thus, a portion of O^* did not participate into methane oxidation, making methane conversion lower [9,12,13,14].

From Fig.4, if H_2O flow was turn off, the activity almost returned to the initial level. This indicated there was a balance of water adsorbed on the catalyst surface at low temperature. When water was turn off, water pressure decreased. H_2O gradually desorbed from the surface and O^* was able to react with CH_4.

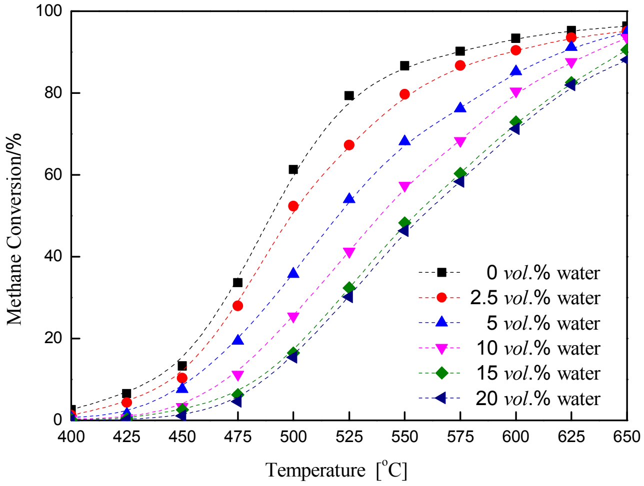

Fig 3. Methane oxidation with water over Cu/γ-Al_2O_3 catalyst (CH_4, 3 *vol.* %; O_2 20 *vol.* %; H_2O, 0-20 *vol.* %; N_2 balance)

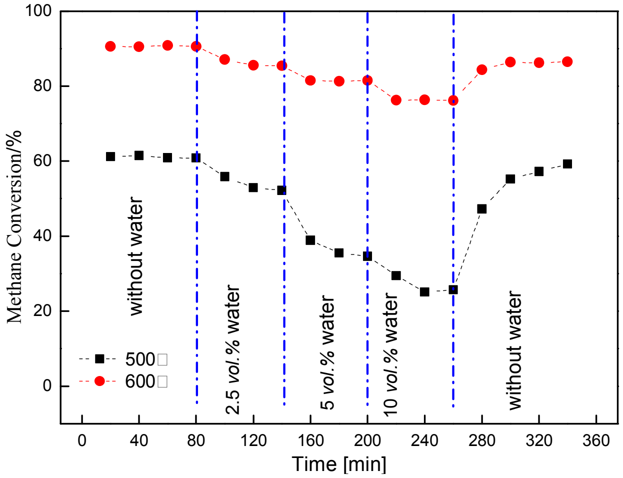

Fig 4. Water inhibitory effect on methane oxidation over Cu/γ-Al_2O_3 catalyst (3 *vol.*% CH_4, 20 *vol.*% O_2)

3.2 Regeneration of Activity of Catalyst

Regeneration of catalytic activity of Cu/γ-Al_2O_3 catalyst was studied by adding water cyclically to the feed gas. By controlling the reaction temperature (500℃,550℃,600℃) and water concentration(2.5 *vol.* %; 5 *vol.* %; 10 *vol.* %), Fig.5 showed the catalyst was purged with N_2. The feed stream was as follows: CH_4, 3 *vol.* %; O_2, 20 *vol.* %; H_2O (2.5 *vol.* %; 5 *vol.* %; 10 *vol.* %); N_2, balance.

In Fig 5, CH_4 conversion was measured by gas chromatography every 15 minutes, whereas the catalyst was purged with nitrogen in the absence of CH_4 for another 10 minutes. Methane conversion was initially high. Then, the activity dropped as water was introduced into the feed gas. Thereafter, the catalyst was purged with N_2 at the same temperature; consequently, no methane was shown in the figure. After purging, activity of catalyst almost recovered to its initial level. Compared with 500℃, 550℃ and 600℃, high temperature weakened the inhibitory effect and activity dropped smaller compared with low temperature. This meant H_2O or surface OH* did not adsorb on the catalyst surface stably, and if temperature increased (500℃→600℃), the process of desorption or decomposition was easy to proceed: $OH^* \rightarrow H_2O + O^*$.

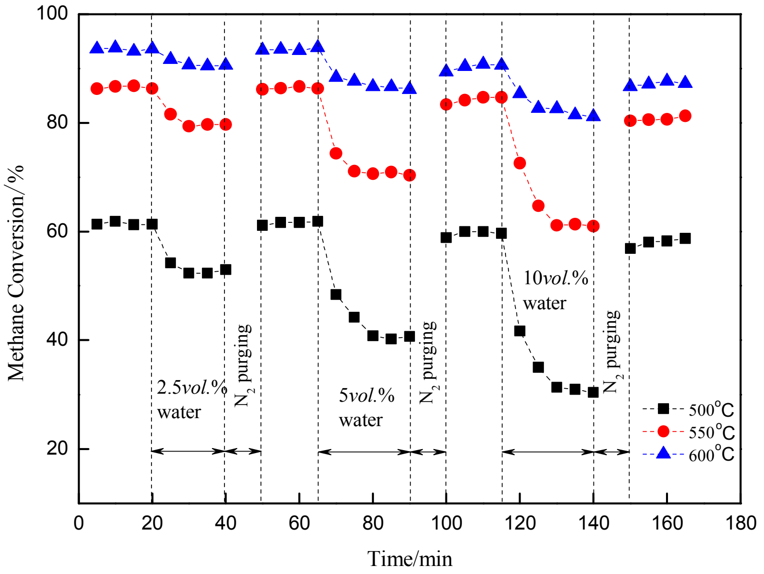

Fig.5 Regeneration of catalytic activity of Cu/γ-Al_2O_3 catalyst (3 *vol.* % CH_4, 20 *vol.* % O_2)

3.3 Surface Characteristics and Stability

In order to discover the influence of water vapor on the catalyst surface, the SEM pictures (1000 times) for the catalyst surface were shown in Fig.6 and BET surface areas (fresh catalyst or the catalyst after the reaction) were shown in Table 3.

In Table 3, the BET surface area of the fresh catalyst was 188.2 m^2/g, while the catalyst after reaction in the dry feed was 180.2 m^2/g. The surface area was reduced by 8.0 m^2/g after reaction. When 5 *vol.* % or 10 *vol.* % vapor was added into the feed, the BET surface area decreased to 166.8 m^2/g and 152.6 m^2/g respectively. Compared with Fig.6 (a) and (b), the sizes of catalyst surface grains were uniformity after the reaction. However, in Fig 6(c) and (d), when 5 *vol.* % and 10 *vol.* % water was introduced into the feed stream, the catalyst grains grew significantly and agglomerate phenomenon occurred obviously.

According to 3.1 and 3.2, activity of Cu/γ-Al_2O_3 catalyst did not recover to its initial level, in spite of high temperature or N_2 purging. The reason might be that the morphology of particles was changing very fast upon this heat and water treatment, and surface deformation blocked the active site. With additional water, it promoted the catalyst surface sintering and some active sites were covered or embedded into the support. Parts of active sites did not interact with methane or oxygen, making activity of Cu/γ-Al_2O_3 catalyst decrease.

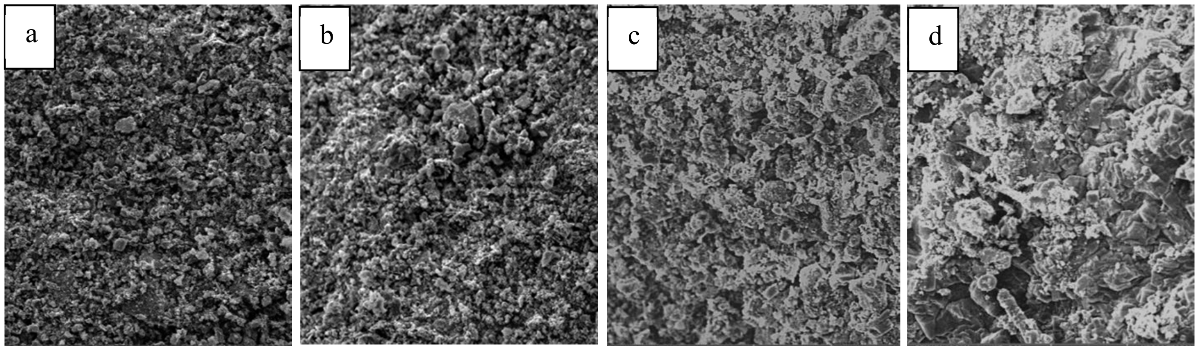

Fig.6 Surface characteristics of Cu/γ-Al_2O_3 catalyst (SEM)

(a) refresh catalyst; (b) catalyst after reaction in the dry feed

(c) catalyst after reaction with 5 *vol.* % water; (d) catalyst after reaction with 10 *vol.* % water

Table 3 BET surface area of the catalyst before or after reaction

Without water		**With water**	
Before reaction	After reaction	5 *vol.%*	10 *vol.%*
188.2(m^2/g)	180.2(m^2/g)	166.8(m^2/g)	152.6(m^2/g)

Fig 7 showed the stability of the activity of Cu/γ-Al_2O_3 catalyst for 42h with or without water. During 42h, when 5 *vol.%* water was introduced into the feed, catalyst maintained high activity for a long time. As the water was turn off, reactivity could recover and maintain stable for 18h.

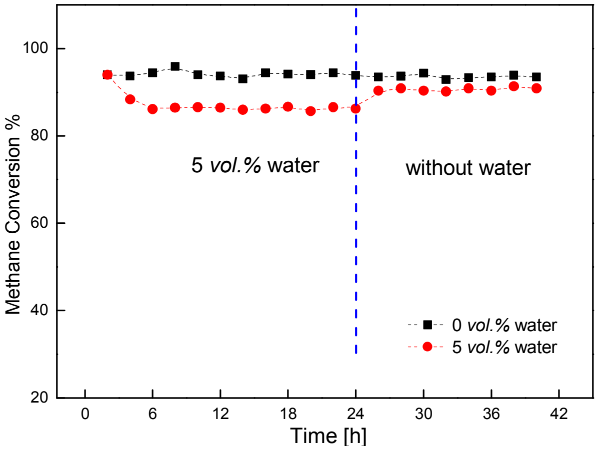

Fig 7. Stability of the activity of Cu/γ-Al_2O_3 catalyst (600℃)

3.4 Apparent Activation Energy of Methane

In order to get the apparent activation energy and kinetic parameters of methane combustion with vapor, we controlled the reaction condition and catalyst to meet the differential condition. Methane conversion required to be limited in a low range (<10%) and catalyst must be diluted to reduce the influence of mass transfer and temperature fluctuation [27,28]. Therefore, we tested the intra-pellet dilution (1:10, 1:15, 1:20, 1:25) and inter-pellet dilution (1:50, 1:75, 1:100) to obtain a suitable dilution ratio to reduce these influence. Fig 8 was the dilution experiment. From Fig 8, when the dilution ratios were 1:20 for intra-pellet dilution and 1:75 for inter-pellet dilution, reaction rate reached to stability. For intra-pellet dilution, 0.05g Cu was choose to load on 1g γ-Al_2O_3, and this catalyst was mixed with 3.75g γ-Al_2O_3 for inter-pellet dilution. The exact values of Cu loading on the support for intra-pellet dilution(1:20) were tested by XRF: Cu, 5.13%; Al, 43.64%; O, 45.63%; Si, 1.43%; K, 1.52%; other, 2.65%. Reaction rate r could be described as:

$$r = F_{CH_4,0} \cdot \frac{x}{W} \tag{2}$$

$F_{CH_4,0}$ and W represented methane input and catalyst mass, respectively.

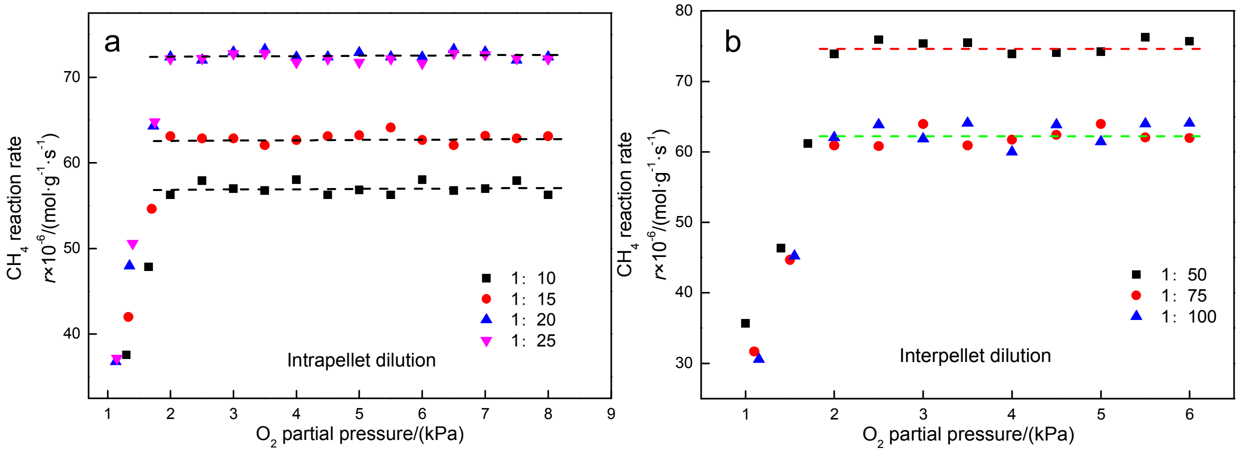

Fig 8. Intra-pellet dilution and Inter-pellet dilution of catalyst (1 *vol.*% CH_4, 400℃)

Temperature was controlled among 360℃～450℃ to limit methane conversion (<10%). The reaction condition was: CH_4, 3 *vol.* %; O_2, 20 *vol.* %; H_2O, 0-10 *vol.* %; N_2 balance. It was generally believed that, unlike the influence of O_2 or CO_2 on combustion in the oxygen-rich condition, water had an obvious effect on activity. The reaction orders with respect to O_2 and CO_2 were zero and to methane was constant, nearly 1.

Fig.9 was the linear fitting result of Arrhenius point of methane combustion with different water concentrations in the feed gas. As no water was introduced into the feed, apparent activation energy (*Ea*) was 81.4 kJ/mol. When H_2O was introduced into the feed (2.5 *vol.* %, 5 *vol.* %, 10 *vol.* %), apparent activation energy (*Ea*) increased: 100.8 kJ/mol, 113.8 kJ/mol, 121 kJ/mol. Water blocked methane oxidation.

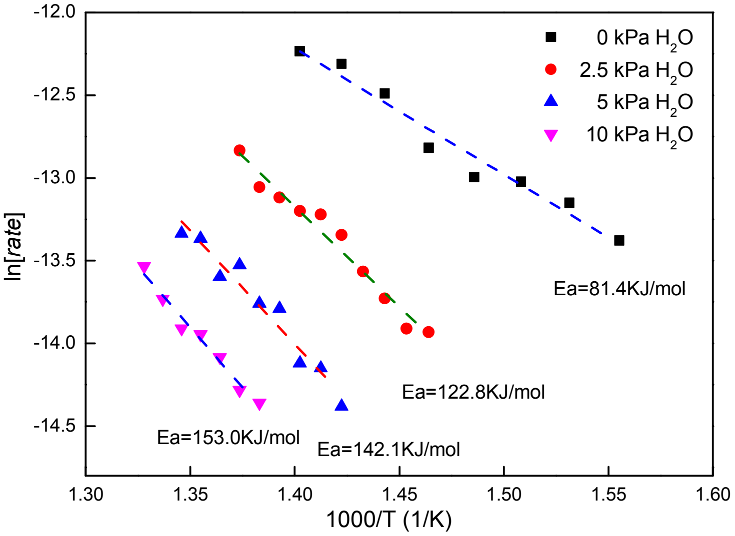

Fig.9 Arrhenius plots of reaction rate vs 1/T for methane combustion. (3 *vol.* % CH_4; 20 *vol.* % O_2) (catalyst intra-pellet dilution, 1:20; catalyst inter-pellet dilution, 1:75)

With the method of Arrhenius point linear fitting, Van Giezen[22] also got the apparent activation energy of methane over Pd catalyst. They controlled the intake flow ratio: CH_4, 1 *vol.* %; O_2, 4 *vol.* %; N_2 balance, H_2O, 0 or 2 *vol.* %, and assumed 0 order reaction orders with respect to oxygen and CO_2, and constant reaction orders with respect to methane (1). Based on the assumptions above, they gained the relationship between reaction order with respect to H_2O and apparent activation energy:

$$E_{A,Dry} = \frac{1}{1-\gamma} E_{A,Wet} \qquad (3)$$

According to the above equation, we calculated reaction order with respect to water: -0.6, -0.796 and -0.911, respectively. Reaction order with respect to water had some decrease as water concentration increased, but the value was within the scope of -0.6～-1 and in agreement with the related reports[22,23]. H_2O influence mainly happened in low temperature (<550℃), in which water adsorbed on O* easily. Apparent activation energy and reaction order with respect to water changed in a certain scope.

3.5 Water Surface Coverage

To explain the adsorption characteristics of vapor on active site, we quote the Langmuir equation to describe water adsorption on the active site. We supposed that the adsorption of methane molecule on active site was the rate-limiting step (oxygen-rich) and methane adsorption on active site was dissociative and irreversible. Water molecular adsorbed on the surface active site, and formed OH* group. OH* could recombine to desorb as H_2O molecule which returned to gaseous phase reactants, generating surface reduced sites. In this process, water and methane molecules were competing for adsorption on the active site. Rate equation could be expressed as:

$$r = k[CH_4]\theta \qquad (4)$$

r was methane reaction rate, k the rate constant, θ the fraction of vacancy sites on the surface, $[CH_4]$ the methane concentration.

Meanwhile, due to the lower partial pressure of methane in the gaseous reactants and rapid consumption with O_2 after adsorption, methane surface coverage was much lower compared to water. Surface active vacancies could be expressed by means of Langmuir isotherm:

$$\theta = 1 - \theta_{H_2O} = 1 - \frac{K_{H_2O}[H_2O]}{1+K_{H_2O}[H_2O]} \qquad (5)$$

$$K_{H_2O} = K_0 \exp\left(\frac{-H_{ads}}{RT}\right) \qquad (6)$$

θ_{H_2O} was water surface coverage on active site, K_{H_2O} and H_{ads} were the water adsorption equilibrium constant and the water adsorption enthalpy, K_0 the pre-exponential factor, $[H_2O]$ the water concentration. When water was introduced into the feed, the expression was:

$$\theta_{H_2O} = \frac{K_{H_2O}([H_2O]_{in}+2x[CH_4]_{in})}{1+K_{H_2O}([H_2O]_{in}+2x[CH_4]_{in})} \qquad (7)$$

$[H_2O]_{in}$ and $[CH_4]_{in}$ were the inlet concentration of water and methane, x the methane conversion.

According to related reports and calculation results of density functional theory [10,11], water adsorption enthalpy(H_{ads}) over Cu catalyst was about -120～-160 kJ/mol and the pre-exponential factor(K_0) was about a magnitude of 10^{10}. Although this was a rough estimate, it obtained a relatively acceptable value of θ_{H_2O} as H_{ads} and K_0 were -160 kJ/mol and 10^{10}, respectively. Calculating by Eq.(7) with parameters, we could obtained water coverage with temperature.

Fig 10 showed water coverage changing with temperature. Water concentrations were: 0 *vol.* %, 2.5 *vol.* %, 5 *vol.* %, 10 *vol.* %. Without water in the feed gas, water coverage was below 30% at 400℃. As water was introduced into the feed, water coverage was above 87% at 400℃. In each condition (water: 2.5 *vol.* %, 5 *vol.* %, 10 *vol.* %), θ_{H_2O} had the same downtrend which tended to 0% when temperature rose up. At low temperature, there was an obvious difference between water coverage with or without water. But at high temperature, the coverage curve tended to the same. High temperature strengthened desorption of water, making water coverage lower.

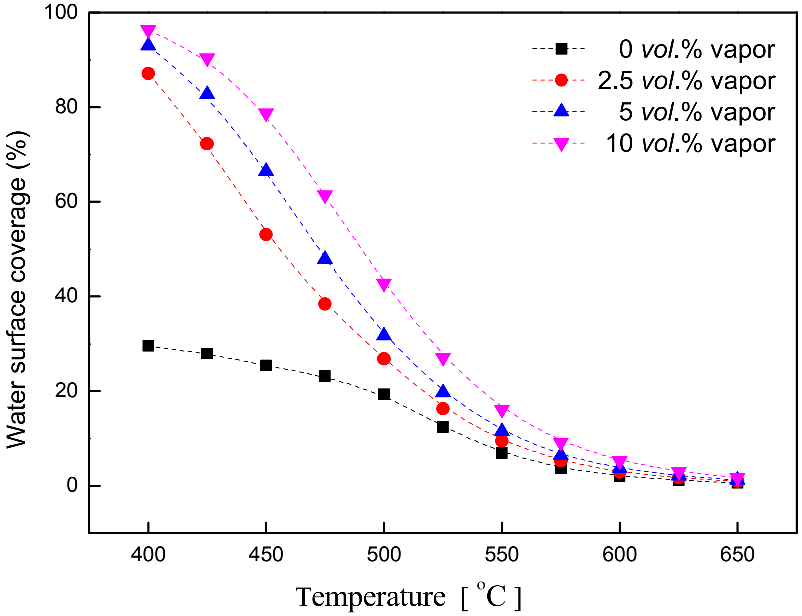

Fig.10 Water coverage vs temperature

(Reaction conditions: CH_4, 3 *vol.* %; O_2, 20 *vol.* %; H_2O, 0-10 *vol.* %; N_2 balance)

4. CONCLUSION

The effect of water on methane combustion over Cu/γ-Al_2O_3 catalyst was investigated in a fixed bed reactor. From the experimental results, we concluded the following points:

1. Combustion efficiency of methane over Cu/γ-Al_2O_3 catalyst was inhibited by H_2O. The inhibitory effect was weakened with temperature rising up. Because of reversible adsorption of water, reactivity could be recovered by N_2 purging which promoted water molecule desorbing from the active site.

2. Water vapor promoted the deformation of catalyst surface, leading to the decrease of surface area and the irreversible effect.

3. The apparent activation energy of methane rose up obviously as vapor was introduced into the feed and the reaction order with respect to vapor maintained among -0.6～-1. Water surface coverage had a downtrend with temperature, which tended to 0% above 625℃.

■AUTHOR INFORMATION

Corresponding Author

Dr. Zhongqing Yang
E-mail address: zqyang@cqu.edu.cn
Full postal address: Room 409, College of Power Engineering, Chongqing University, Shapingba Dist. Chongqing, P. R. China, 400030
TEL: 86-23-65103114

ACKNOWLEDGMENT

The authors would like to thank the financial supports of Natural Science Foundation of China with Project No.51206200, and the Fundamental Research Funds for the Central Universities with Project No.

CDJZR12140031, and visiting Scholar Foundation of Key Lab. of Low-grade Energy Utilization Technologies and System, MOE of China in Chongqing University(LLEUTS-201301).

REFERENCES

[1] Tao Kai, Zhou Shenghu, Zhang Qiuju, et al. Sol-gel auto-combustion synthesis of Ni-$Ce_xZr_{1-x}O_2$ catalysts for carbon dioxide reforming of methane [J]. RSC Advances, 2013, 3(44): 22285-22294.

[2] Zhongqing Yang, John. R. Grace, C. Jim Lim, Li Zhang. Combustion of low-concentration coal bed methane in a fluidized bed reactor [J]. Energy & Fuels, 2011, 25(3): 975-980.

[3] Yang Z, Liu J, Zhang L, et al. Catalytic combustion of low-concentration coal bed methane over CuO/γ-Al_2O_3 catalyst: effect of SO_2[J]. RSC Advances, 2014, 4(74): 39394-39399.

[4] Bhavsar Saurabh, Veser Gtz. Chemical looping beyond combustion: Production of synthesis gas via chemical looping partial oxidation of methane [J]. RSC Advances, 2014, 4(88): 47254-47267.

[5] Guo Guangsheng, Lian Kuo, Wang Lijuan, Gu Fubo, et al. High specific surface area $LaMO_3$ (M = Co, Mn) hollow spheres: Synthesis, characterization and catalytic properties in methane combustion [J]. RSC Advances, 2014, 4(102): 58699-58707.

[6] Eriksson S, Boutonnet M, Järås S. Catalytic combustion of methane in steam and carbon dioxide-diluted reaction mixtures[J]. Applied Catalysis A: General, 2006, 312(8): 95-101.

[7] Dupont V, Zhang S H, Bentley R, et al. Experimental and modelling studies of the catalytic combustion of methane[J]. Fuel, 2002, 81(6): 799-810.

[8] Hu Xun, Zhang Lijun, Dong Dehua, Lu Gongxuan. High-temperature steam reforming of bio-oil derived light organics and methane to hydrogen-rich gas with trace CO via rational temperature control [J]. RSC Advances, 2014, 4(36): 18924-18929.

[9] Gélin P, Urfels L, Primet M, et al. Complete oxidation of methane at low temperature over Pt and Pd catalysts for the abatement of lean-burn natural gas fuelled vehicles emissions: influence of water and sulphur containing compounds[J]. Catalysis today, 2003, 83(1): 45-57.

[10] Nagase K, Zheng Y, Kodama Y, et al. Dynamic Study of the Oxidation State of Copper in the Course of Carbon Monoxide Oxidation over Powdered CuO and Cu_2O[J]. Journal of Catalysis, 1999, 187(1): 123-130.

[11] Shinde Vijay M, Madras Giridhar. Catalytic performance of highly dispersed Ni/TiO_2 for dry and steam reforming of methane [J]. RSC Advances, 2014, 4(10), 4817-4826.

[12] GAO D, WANG S, ZHANG C, et al. Methane Combustion over Pd/Al_2O_3 Catalyst: Effects of Chlorine Ions and Water on Catalytic Activity[J]. Chinese Journal of Catalysis, 2008, 29(12): 1221-1225.

[13] Kikuchi R, Maeda S, Sasaki K, et al. Low-temperature methane oxidation over oxide-supported Pd catalysts: inhibitory effect of water vapor[J]. Applied Catalysis A: General, 2002, 232(1): 23-28.

[14] Araya P, Guerrero S, Robertson J, et al. Methane combustion over Pd/SiO_2 catalysts with different degrees of hydrophobicity[J]. Applied Catalysis A: General, 2005, 283(1): 225-233.

[15]Hu X, Yu Q, Sun N, et al. Experimental study of flammability limits of oxy-methane mixture and calculation based on thermal theory[J]. International Journal of Hydrogen Energy, 2014, 39(17): 9527-9533.

[16] Ciuparu D, Perkins E, Pfefferle L. In situ DR-FTIR investigation of surface hydroxyls on γ-Al_2O_3 supported PdO catalysts during methane combustion[J]. Applied Catalysis A: General, 2004, 263(2): 145-153.

[17] Ciuparu D, Pfefferle L. Support and water effects on palladium based methane combustion catalysts[J]. Applied Catalysis A: General, 2001, 209(1): 415-428.

[18] Stasinska B, Machocki A, Antoniak K, et al. Importance of palladium dispersion in Pd/Al_2O_3 catalysts for complete oxidation of humid low-methane–air mixtures[J]. Catalysis Today, 2008, 137(2): 329-334.

[19] Ong Wee-Jun, Gui Meei Mei, Chai Siang-Piao, et al. Direct growth of carbon nanotubes on Ni/TiO_2 as next generation catalysts for photoreduction of CO_2 to methane by water under visible light irradiation [J]. RSC Advances, 2013, 3(14): 4505-4509.

[20] Qiao D, Lu G, Guo Y, et al. Effect of water vapor on the CO and CH4 catalytic oxidation over CeO2-MOx (M= Cu, Mn, Fe, Co, and Ni) mixed oxide[J]. Journal of Rare Earths, 2010, 28(5): 742-746.

[21] Wu Tao, Cai Weiye, Zhang Peng, et al. Cu-Ni@SiO_2 alloy nanocomposites for methane dry reforming catalysis [J]. RSC Advances, 2013, 3(46): 23976-23979.

[22] Van Giezen J C, Van den Berg F R, Kleinen J L, et al. The effect of water on the activity of supported palladium catalysts in the catalytic combustion of methane[J]. Catalysis today, 1999, 47(1): 287-293.

[23] Águila G, Gracia F, Cortés J, et al. Effect of copper species and the presence of reaction products on the activity of methane oxidation on supported CuO catalysts[J]. Applied Catalysis B: Environmental, 2008, 77(3): 325-338.

[24] Pieck C L, Vera C R, Peirotti E M, et al. Effect of water vapor on the activity of Pt-Pd/Al_2O_3 catalysts for methane combustion[J]. Applied Catalysis A: General, 2002, 226(1): 281-291.

[25] Ozawa Y, Tochihara Y, Nagai M, et al. PdO/Al_2O_3 in catalytic combustion of methane: stabilization and deactivation[J]. Chemical Engineering Science, 2003, 58(3): 671-677.

[26] Persson K, Pfefferle L D, Schwartz W, et al. Stability of palladium-based catalysts during catalytic combustion of methane: The influence of water[J]. Applied Catalysis B: Environmental, 2007, 74(3): 242-250.

[27] Chin Y H, Buda C, Neurock M, et al. Reactivity of chemisorbed oxygen atoms and their catalytic consequences during CH_4–O_2 catalysis on supported Pt clusters[J]. Journal of the American Chemical Society, 2011, 133(40): 15958-15978.

[28] Xu J, Ouyang L, Mao W, et al. Operando and Kinetic Study of Low-Temperature, Lean-Burn Methane Combustion over a Pd/γ-Al_2O_3 Catalyst[J]. ACS Catalysis, 2012, 2(2): 261-269.